

cant and are also shown in Fig. 3.  $M$  increases as the temperature is lowered, and attains saturation for  $T < 60$  K. There is no magnetization compensation for this alloy in the range of temperatures studied here.  $Ku$  increases as the  $T$  is lowered and more so for  $T < 80$  K. In Tb-Fe alloys, besides the one ion contribution from Tb there could also be a strong contribution from magnetoelastic interaction. It has recently<sup>6</sup> been shown that, for a composition of  $Tb_{26}Fe_{74}$ , most of the measured  $Ku$  could be attributed to the magnetoelastic energy. So the measured  $Ku = Ku' + Ku$  (ME), where  $Ku'$  is the random one ion anisotropy<sup>2</sup> and  $Ku$  (ME) =  $-3/2 \sigma \lambda$ , where  $\sigma$  is the stress and  $\lambda$  the magnetostriction. The sputtered films, in general, are in compression ( $\sigma < 0$ ) and  $\lambda > 0$ , therefore,  $Ku$  (ME)  $> 0$  and, hence, additive. As the temperature is lowered, due to the stronger contraction of metallic film as compared to that of the glass substrate, the film would experience more and more tension ( $\sigma' > 0$ ) and, hence, lesser compressive stress. As the initial value of  $\sigma$  is itself strongly dependent on Ar pressure, this parameter will greatly influence the situation at low  $T$ . Because  $\lambda$  would strongly increase at low  $T$ , this could compensate for the eventual decrease in the compressive stress. If the resultant stress at low  $T$  were to become a tensile one ( $\sigma' > 0$ ) then  $Ku$ (ME) would even change the sign, thereby decreasing the measured  $Ku$ . Our results show that  $Ku$  is still increasing strongly at lower  $T$ . This could mean that  $Ku$ (ME) is still

positive and is additive. Under these circumstances, it is not easy to verify the theoretical models for the temperature dependence of  $Ku$ . Our results would show that  $Ku$  varies as  $M^3$  which could be fortuitous as well. Our analysis would then explain why, in some cases,  $Ku$  tends to decrease or change signs at low temperatures. Since the type of sputtering techniques (rf diode, triode, and planar magnetron), are known to strongly affect the microstructure, it is hazardous to generalize the results. To be able to test the theory it would be necessary to work on compositions where  $\lambda$  is negligible, which means that Tb may not be the best candidate. One could also envisage, preparing samples with minimum residual stress, by properly choosing the sputtering conditions. Work on these lines is being planned for the future.

<sup>1</sup>Y. Togami, IEEE Trans. Magn. MAG-18, 1233 (1982).

<sup>2</sup>R. W. Cochrane, R. Harris, and M. J. Zuckermann, Phys. Rep. 48, 1 (1978).

<sup>3</sup>R. B. van Dover, M. Hong, E. M. Gyorgy, J. F. Dillon, and S. D. Alibiston, J. Appl. Phys. 57, 3897 (1985).

<sup>4</sup>H. Miyajima, K. Sato, and T. Mizoguchi, J. Appl. Phys. 47, 4669 (1976).

<sup>5</sup>W. H. Meiklejohn, F. E. Luborsky, and P. G. Frischmann, INTERMAG '87, Tokyo, paper no. BB-05.

<sup>6</sup>S. Hashimoto, Y. Ochi, M. Kaneko, K. Watanabe, and K. Aso, INTERMAG '87, Tokyo, paper no. BB-07.

## Ion mixing and thermochemical properties of tracers in Ag

E. Ma, S.-J. Kim, and M.-A. Nicolet

*Applied Physics and Electrical Engineering, 116-81, California Institute of Technology, Pasadena, California 91125*

R. S. Averbach

*Department of Materials Science, University of Illinois at Urbana-Champaign, Urbana, Illinois 61801*

(Received 9 November 1987; accepted for publication 3 December 1987)

Very thin films of Ni, Ta, W, Pb, and Bi in a Ag matrix were irradiated at 77 K with 330 keV Kr ions at doses from 3 to  $7 \times 10^{15}$  ions/cm<sup>2</sup> and analyzed at room temperature by backscattering of 1.9 MeV He<sup>+</sup>. The measured mixing efficiencies,  $Dt/\phi F_D$ , for the various tracers correlate with their respective tracer impurity diffusion coefficients and impurity-vacancy binding energies in Ag. The results concur with previous ones with a Cu matrix and further support the idea that the parameters that are important for thermal diffusion are also important for ion mixing in a thermal spike.

It is well established that for low temperature ion mixing, a thermal spike mechanism can contribute significantly to the atomic displacements.<sup>1-3</sup> The degree to which other mechanisms also contribute depends on the various parameters of target and impinging ions. For irradiation with light ions of target systems with high cohesive energy and low mass, the cascade energy density is small and the collisional mechanism is expected to play an important role as the thermal spike mechanism. For a dense cascade, however, the thermal spike mechanism dominates.<sup>3-5</sup>

We investigate the effect of the thermal spike mechanism for ion mixing of tracers in Ag. It has been previously<sup>6</sup> shown that the ion mixing results of tracers in Cu correlate with the thermal diffusion of tracer impurities and the vacancy-impurity atom binding energies in Cu. These findings suggest that the transport mechanism in a thermal spike is related to that of thermal diffusion. Ag, like Cu, has a low cohesive energy, which favors the creation upon irradiation of high point defect concentrations with high defect mobilities.<sup>4</sup> Ag also favors cascades with high energy density which

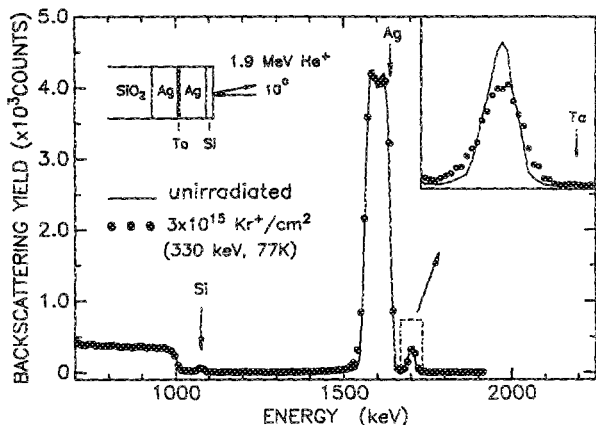


FIG. 1. Typical 1.9 MeV  $\text{He}^+$  backscattering spectra showing the spreading of a Ta tracer in Ag matrix.

lead to a high effective cascade temperature and perhaps even to melting.<sup>4,7</sup> These factors promote thermal spike diffusion. Furthermore, Ag is isoelectronic with Cu. Thus, the importance of thermochemical properties in ion mixing can be further tested with Ag.

The tracer marker samples were prepared on thick ( $\sim 1 \mu\text{m}$ )  $\text{SiO}_2$  layers grown on Si wafers by thermal oxidation. These inert substrates were used to prevent interactions between the sample and the substrate during irradiation. The vacuum was better than  $2 \times 10^{-7}$  Torr during evaporation. Ag matrices and tracers were deposited sequentially without breaking the vacuum. The elements Ni, Ta, W, Pb, and Bi were selected as tracers because their diffusivities in Ag span a wide range of values. The tracers had nominal thicknesses of  $\sim 10 \text{ \AA}$  and were located at the mid-plane of the 600  $\text{ \AA}$  thick Ag. All samples were covered with a layer of about 40  $\text{ \AA}$  Si to minimize reactions with the ambient gas and to reduce sputtering. The samples were irradiated at 77 K with 330 keV Kr to doses ranging from 3 to  $7 \times 10^{15} \text{ Kr/cm}^2$  and analyzed at room temperature with 1.9 MeV  $\text{He}^+$  backscattering spectrometry. The analyzing beam was incident along sample normal and had a typical spot size of a few  $\text{mm}^2$ . The scattering angle was  $170^\circ$ .

TABLE I. Compilation of ion mixing results for tracers in Ag matrix.

Tracer in Ag	$D_i/\phi$ $F_D (\text{ \AA}^2/\text{eV})$	Source	$D_{th}$ $(10^6 \text{ \AA}^2/\text{s})$	$H_b$ $(\text{kJ/mol})$
W	19 <sup>a</sup>	This work	...	-62
Ta	25 <sup>a</sup>	This work	...	-47
Pt	59 <sup>b</sup>	Ref. 5	5	-23
Ni	83 <sup>a</sup>	This work	44	-18
Cu	138 <sup>c</sup>	Ref. 10	84	-5
Al	93 <sup>b</sup>	Ref. 5	232	-2
Pb	> 160 <sup>a</sup>	This work	402	6
Bi	> 160 <sup>a</sup>	This work	$\sim 400$	7

<sup>a</sup> Value used for  $F_D$  for 330 keV Kr at the depth of the tracer layer in Ag was  $212 \text{ eV/\AA}$ , as calculated from the computer simulation, TRIM.

<sup>b</sup> The samples were irradiated with 650 keV Kr at 7 K with *in situ* backscattering analysis.  $F_D$  at the depth of the tracer layer was  $197 \text{ eV/\AA}$ .

<sup>c</sup> The samples were irradiated with 750 keV Kr at 77 K with *in situ* analysis.  $F_D$  at the depth of the tracer layer was  $146 \text{ eV/\AA}$ .

Typical backscattering spectra for a Ta tracer are shown in Fig. 1. The sample configuration is depicted in the insert of the figure. The observed tracer signals are fitted well by Gaussian profiles. The difference in the variances of these fits to the tracer signals in the spectra before and after the irradiation,  $2Dt$ , is taken as measure of the mixing, as described in detail elsewhere.<sup>8</sup> The data for  $2Dt$  are then converted to mixing efficiency by dividing by  $2\phi F_D$ , where  $\phi$  is the dose, and  $F_D$  is the deposited damage energy-per-unit length normal to the surface. Values of  $F_D$ , calculated from a computer simulation TRIM,<sup>9</sup> are given in the footnotes of Table I. The measured variances  $2Dt$  for most of the samples increased linearly with dose. The measured mixing efficiencies are summarized in Table I, with additional data from Refs. 5 and 10. The data from the references have been obtained under experimental conditions somewhat different from the present ones (also see the footnotes of Table I for details). These differences, namely the irradiation at 7 K rather than at 77 K or the *in situ* analysis rather than at room temperature, are known to have very small effects on ion mixing efficiency.<sup>5,6,11</sup> The table also includes the two parameters that we try to correlate with ion mixing, namely the thermal tracer impurity diffusion coefficient in Ag,  $D_{th}$ , and the vacancy-impurity binding energy in Ag,  $H_b$ .

The samples containing Pb and Bi tracers are unusual in that these tracers undergo significant diffusion through the Ag already in the as-deposited samples without irradiation. The backscattering spectra revealed that in these samples two additional tracer peaks arising from Pb (or Bi) appeared at the  $\text{SiO}_2$  substrate/Ag interface and the sample surface, respectively. This impurity distribution is characteristic of grain boundary diffusion.<sup>12,13</sup> After the lowest irradiation dose of  $3 \times 10^{15} \text{ Kr/cm}^2$ , most of the tracer atoms near the sample surface are sputtered off, while the other two tracer peaks broaden widely and overlap. Gaussians were fitted to these barely discernible tracer signal peaks. The ion mixing amounts so derived, however, contain large uncertainties. Thus, we have quoted in Table I only a minimum value for the mixing efficiencies of these two tracers in Ag.

The tracer impurity diffusion coefficient values in Ag,  $D_{th}$ , indicated in the table were obtained by extrapolating the literature data<sup>14</sup> to the melting point of Ag ( $T_0 = 1234 \text{ K}$ ). We were not able to find the diffusivities for W, Ta, and Bi in Ag. The diffusivity of Bi in Ag was assumed to be similar to that of Pb in Ag since these two tracers have similar atomic properties.

A comparison of the thermal diffusion coefficients and the tracer ion mixing efficiencies in Table I shows that as the impurity thermal diffusion increases, the ion beam induced mixing also increases. This trend suggests a correlation between the two phenomena. It has been shown both conceptually<sup>1,15</sup> and experimentally<sup>5,6</sup> that during ion mixing in a thermal spike, thermally aided processes for atomic displacements are significant. In Ref. 15, a thermal spike model was proposed that explicitly shows a connection between the thermal diffusion of an impurity and ion mixing. In this model the high concentration of point defects created in the collisional phase of the cascade enhances the diffusion at the transiently high temperatures of the thermal spike. This is

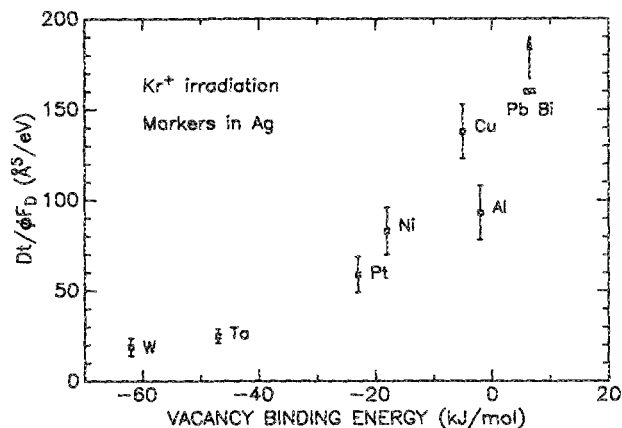


FIG. 2. Vacancy-impurity binding energies of tracers in Ag,  $H_b$ , as a function of the mixing efficiencies,  $Dt/\phi F_D$ .

the reason why we quote  $D_{th}$  in Table I at the melting point of Ag. The scatter in the trend between the thermal diffusion and the mixing efficiency can be attributed, at least partly, to the extrapolation of  $D_{th}$  to the melting point of Ag, and to the fact that the point defect concentration in the highly transient state of the thermal spike differs from that under the condition of thermal equilibrium. In Refs. 5 and 7, it is suggested that melting may occur during the thermal spike. In such a case, tracer diffusion coefficients in liquid Ag could be more appropriate. The diffusion coefficient data in liquid Ag for many of our tracers are not available in literature. However, a brief survey of the available data<sup>16</sup> suggest that the tracer impurity diffusion coefficients in liquid Ag (e.g., the activation energy) behave similarly to those in solid Ag. Such a correlation has also been noted in the case of Cu.<sup>5,7</sup> Although the theory of diffusion in liquids is not well founded, it is not surprising that impurity diffusions in a liquid metal and in the solid metal at the melting point are alike. Thus, the data would be consistent with a point defect model of diffusion in a cascade or liquid diffusion.

If the ion mixing mechanism is indeed related to that of the thermal diffusion in solid Ag, then the mixing efficiencies should also correlate with the point defect properties that are germane to the thermal diffusion of the impurities. It is known<sup>17</sup> that the vacancy mechanism is dominant for impurity diffusion in Ag. Thus, from the electrostatic diffusion theory<sup>17,18</sup> an impurity with positive excess valency in Ag, such as Al, Pb, or Bi should mix more than those with negative valency such as Ni, Ta, W, and Pt. We indeed, observe such a trend from Table I, suggesting that the vacancy mechanism is important during ion mixing. To further substantiate this observation, we have tried to correlate the mixing efficiencies with the vacancy-impurity binding energy,  $H_b$ .  $H_b$  was calculated from the approximate empirical formulas

of Ref. 19:  $H_b = (H_A - H_B - H^s)/Z_0$ , where  $H_A$  and  $H_B$  are the cohesive energies of the solvent and solute atoms,<sup>20</sup>  $H^s$  is the heat of solution,<sup>21</sup> and  $Z_0$  is the number of nearest neighbors in Ag ( $= 12$ ). The  $H_b$  values we obtained are also listed in Table I. In Fig. 2, the mixing efficiency of each tracer is plotted against the vacancy-impurity binding energy  $H_b$ . If the vacancy mechanism dominates during a thermal spike phase of ion mixing, then large mixing efficiencies should correlate with large positive  $H_b$ , while the small mixing efficiencies should correlate with large negative  $H_b$ . Figure 2 does indeed, establish such a correlation, again indicating that a mechanism important during thermal diffusion is also important during the thermal spike phase of ion mixing.

In conclusion, this experiment for a Ag matrix corroborates the results obtained for a Cu matrix<sup>6</sup> and lends further support to the notion that for ion irradiation at low temperatures, the ion mixing in the thermal spike correlates with the thermal diffusion properties in the metal, whether the metal be solid or liquid.

We are grateful to R. Gorris at Caltech for technical assistance. This work was supported at Caltech by The Office of Naval Research under Contract No. N00014-84-K-0275 and at the University of Illinois by the Department of Energy under Contract No. DEAC02-76ER01198.

- <sup>1</sup>G. H. Vineyard, *Radiat. Eff.* **29**, 245 (1976).
- <sup>2</sup>M. W. Guinan and J. H. Kinney, *J. Nucl. Mater.* **103/104**, 1319 (1981).
- <sup>3</sup>W. L. Johnson, Y.-T. Cheng, M. Van Rossum, and M.-A. Nicolet, *Nucl. Instrum. Methods B* **7/8**, 657 (1985).
- <sup>4</sup>R. S. Averback, *Nucl. Instrum. Methods B* **15**, 675 (1986).
- <sup>5</sup>S.-J. Kim, M.-A. Nicolet, and R. S. Averback, *Phys. Rev. B* (in press).
- <sup>6</sup>S.-J. Kim, M.-A. Nicolet, and R. S. Averback, *Appl. Phys. A* **41**, 171 (1986).
- <sup>7</sup>T. D. dela Rubia, R. S. Averback, R. Benedek, and W. E. King, *Phys. Rev. Lett.* (in press).
- <sup>8</sup>S.-J. Kim, M.-A. Nicolet, R. S. Averback, and P. Baldo, *Appl. Phys. Lett.* **46**, 154 (1985).
- <sup>9</sup>J. Biersack and L. G. Haggmark, *Nucl. Instrum. Methods* **174**, 257 (1980).
- <sup>10</sup>S.-J. Kim, M.-A. Nicolet, and R. S. Averback (unpublished).
- <sup>11</sup>B. M. Paine and R. S. Averback, *Nucl. Instrum. Methods B* **7/8**, 666 (1985).
- <sup>12</sup>P. G. Shewmon, *Diffusion in Solids* (McGraw-Hill, New York, 1963), Chap. 6.
- <sup>13</sup>K. N. Tu, *J. Appl. Phys.* **43**, 1303 (1972).
- <sup>14</sup>C. J. Smithells, Ed., *Metals Reference Book*, 5th ed. (Butterworths, London, 1976), pp. 13 and 14.
- <sup>15</sup>D. Peak and R. S. Averback, *Nucl. Instrum. Methods B* **7/8**, 561 (1985).
- <sup>16</sup>F. H. Wohlbiel, Ed., *Diffusion and Defect Data*, Vols. 1-42 (Trans. Tech. S. A., Aedermannsdorf, Switzerland, 1969-1985).
- <sup>17</sup>A. D. Le Claire, *Philos. Mag.* **7**, 141 (1962).
- <sup>18</sup>D. Lazarus, *Phys. Rev.* **93**, 973 (1954).
- <sup>19</sup>A. Seeger, *Lattice Defects and Their Interaction*, edited by R. R. Hasiguti (Gordon and Breach, New York, 1962), p. 181.
- <sup>20</sup>C. Kittel, *Introduction to Solid State Physics*, 5th ed. (Wiley, New York, 1976), p. 74.
- <sup>21</sup>A. K. Niessen, F. R. de Boer, R. Boom, P. F. de Chatel, and W. C. M. Mattens, *Calphad* **7**, 51 (1983).